

NFAT1 Hypermethylation Promotes Epithelial-Mesenchymal Transition and Metastasis in Nasopharyngeal Carcinoma by Activating *ITGA6* Transcription^{1,2}



Jian Zhang^{*,†,3}, Zi-Qi Zheng^{*,3}, Ya-Wei Yuan^{†,3},
Pan-Pan Zhang^{*,3}, Ying-Qin Li^{*,}, Ya-Qin Wang^{*,},
Xin-Ran Tang^{*,}, Xin Wen^{*,}, Xiao-Hong Hong^{*,},
Yuan Lei^{*,}, Qing-Mei He^{*,}, Xiao-Jing Yang^{*,},
Ying Sun^{*,}, Jun Ma^{*,} and Na Liu^{*,}

* State Key Laboratory of Oncology in South China, Collaborative Innovation Center of Cancer Medicine, Guangdong Key Laboratory of Nasopharyngeal Carcinoma Diagnosis and Therapy, Sun Yat-sen University Cancer Center, Guangzhou, 510060, PR China; [†] Department of Radiation Oncology, Affiliated Cancer Hospital & Institute of Guangzhou Medical University, Guangzhou 510095, PR China

Abstract

DNA methylation is an important epigenetic change in carcinogenesis. However, the function and mechanism of DNA methylation dysregulation in nasopharyngeal carcinoma (NPC) is still largely unclear. Our previous genome-wide microarray data showed that *NFAT1* is one of the most hypermethylated transcription factor genes in NPC tissues. Here, we found that *NFAT1* hypermethylation contributes to its down-regulation in NPC. *NFAT1* overexpression inhibited cell migration, invasion, and epithelial-mesenchymal transition *in vitro* and tumor metastasis *in vivo*. We further established that the tumor suppressor effect of *NFAT1* is mediated by its inactivation of *ITGA6* transcription. Our findings suggest the significance of activating *NFAT1/ITGA6* signaling in aggressive NPC, defining a novel critical signaling mechanism that drives NPC invasion and metastasis and providing a novel target for future personalized therapy.

Neoplasia (2019) 21, 311–321

Introduction

Nasopharyngeal carcinoma (NPC) is a malignant tumor with the highest incidence rate in Southern China and Southeast Asia [1–3]. Recent advances in intensity-modulated radiotherapy and the application of chemoradiotherapy have greatly improved prognosis, but approximately 30% of NPC patients eventually develop recurrence and/or distant metastasis [4]. Therefore, better understanding the underlying molecular mechanisms that regulate NPC metastasis is essential for the development of novel treatment strategies for NPC patients.

Epigenetic modification, including DNA methylation, can change gene expression without altering nucleotide sequence. Aberrant DNA methylation plays a vital role in carcinogenesis and progression of cancers, and its dynamic nature and reversible changes make it a meritorious target for cancer treatment [5,6]. Accumulating evidence demonstrates that hypermethylation in the promoter region of genes is a major mechanism involved in the inactivation or silencing of tumor suppressor genes (TSGs) in various cancers [7–10]. It has also been reported that promoter hypermethylation of TSGs is a common

Address all correspondence to: Na Liu, State Key Laboratory of Oncology in South China, Sun Yat-sen University Cancer Center, 651 Dongfeng Road East, Guangzhou 510060, PR China. E-mail: liun1@sysucc.org.cn

¹ Acknowledgements: This work was supported by grants from the National Natural Science Foundation of China (81802920), the Guangdong Special Support Program (2017TQ04R754), the Natural Science Foundation of Guang Dong Province (2018B030306045, 2017A030312003), the Health & Medical Collaborative Innovation Project of Guangzhou City, China (201803040003), the Innovation Team Development Plan of the Ministry of Education (IRT_17R110), the Overseas Expertise Introduction Project for Discipline Innovation (111 Project, B14035), the Young Talents Project of Sun Yat-sen Cancer Center (16zxc15) and the Guangzhou Key Medical Discipline Construction Project Fund (B185006004035).

² The authors declare that they have no competing interests.

³ Jian Zhang, Zi-Qi Zheng, Ya-Wei Yuan and Pan-Pan Zhang contributed equally to this article.

Received 31 August 2018; Revised 17 January 2019; Accepted 23 January 2019

© 2019 The Authors. Published by Elsevier Inc. on behalf of Neoplasia Press, Inc. This is an open access article under the CC BY-NC-ND license (<http://creativecommons.org/licenses/by-nc-nd/4.0/>).
1476-5586
<https://doi.org/10.1016/j.neo.2019.01.006>

event in NPC [11,12]. Dai et al. found that almost 91% of differentially methylated CpG sites in NPC were hypermethylated [13]. These findings suggest that TSG hypermethylation may play critical roles in NPC development and progression, and further studies are warranted to elucidate their functions and mechanisms.

Our previous genome-wide methylation study identified nuclear factor of activated T cells (*NFAT1*) as one of the top-ranked hypermethylated transcription factor genes in NPC [14]. NFAT1, also known as NFATc2/NFATp, can modulate cellular transformation by regulating the expression of cell cycle-related proteins [15–17] and can play a tumor-suppressor role by reversing the transformed phenotype of neoplastic cells [18–20]. However, the role and mechanism of NFAT1 remains unclear in NPC. In this study, we demonstrate that promoter hypermethylation of *NFAT1* contributes to its down-regulation in NPC, thereby promoting NPC cell epithelial-mesenchymal transition (EMT) and metastasis by activating the transcription of integrin subunit alpha 6 (*ITGA6*). Our findings reveal the role of NFAT1/*ITGA6* signaling in NPC, providing novel therapeutic targets for individualized NPC therapy.

Materials and Methods

Cell Culture and Clinical Specimens

Human NPC cell lines (CNE1, CNE2, SUNE1, HONE1, HNE1, 5-8F, and 6-10B) were cultured in Roswell Park Memorial Institute (RPMI)-1640 (Invitrogen, USA) supplemented with 10% fetal bovine serum (FBS; Gibco). Normal human nasopharyngeal epithelial cell lines (NP69 and N2-Tert) were grown in Keratinocyte Serum Free Medium (Invitrogen) supplemented with bovine pituitary extract (BD Biosciences, San Jose, CA). HEK-293 T cells were cultured in Dulbecco's modified Eagle's medium (DMEM; Invitrogen) supplemented with 10% FBS. Nasopharyngeal epithelial and NPC cell lines were treated with or without 10 $\mu\text{mol/L}$ 5-aza-2'-deoxycytidine (DAC; Sigma-Aldrich) for 72 h, with the drug/media replaced every 24 h. Twenty-seven freshly-frozen NPC and 23 normal nasopharyngeal epithelium tissue samples were collected from Sun Yat-sen University Cancer Center. This study was authorized by the Institutional Ethical Review Boards of Sun Yat-sen University Cancer Center, and written informed consents were provided by all patients for use of their biopsy tissue samples.

Plasmids, Virus Production, and Transfection

The pSin-EF2-puro-*NFAT1*-HA or pSin-EF2-puro-vector plasmids were obtained from Land Hua Gene Biosciences. pEnter-*ITGA6*-HIS and pEnter-vector plasmids were obtained from Vigene Bioscience. The short hairpin RNA targeting *NFAT1* (*shNFAT1*) (Table S1) was synthesized and then cloned into pLKO.1-puromycin-GFP. For transient transfection, plasmids (2 μg) were transfected with Lipofectamine 2000 reagent (Invitrogen) and then harvested for assays 48 h after transfection. To generate stably transfected cell lines, lentivirus assembly expression plasmids were co-transfected into 293 T cells. Virus-containing supernatants were used to infect NPC cells for 48 h, and stable clones were selected using 0.5 $\mu\text{g/ml}$ puromycin. The transduction efficiency was validated using RT-PCR and Western blot assays.

DNA Isolation and Bisulfite Pyrosequencing Analysis

DNA from NPC tissues or cell lines was isolated using the AllPrep RNA/DNA Mini Kit (Qiagen, USA) or EZ1 DNA Tissue Kit (Qiagen), and 1–2 μg DNA was then treated with sodium bisulfite

using the EpiTect Bisulfite kit (Qiagen) according to the manufacturer's instructions. Bisulfite pyrosequencing primers are shown in Table S1. The PyroMark Q96 System (Qiagen) was used for the sequencing reactions and methylation level quantification.

Quantitative Reverse Transcription (RT)-PCR

Total RNA from NPC cell lines and tissues was isolated with TRIzol reagent (Invitrogen) as instructed. cDNA was synthesized using a Reverse Transcription Kit (Promega, Madison, WI). Quantitative analysis was performed using SYBR Green Real-Time PCR Master Mix Kit (Invitrogen). The experiments were performed in triplicate for each sample and normalized to expression of the housekeeping gene *GAPDH*. The analysis was calculated by relative quantification ($2^{-\Delta\Delta\text{CT}}$). The primer sequences are shown in Table S1.

Western Blot

Total protein was extracted using RIPA buffer, and then quantified using Pierce BCA protein assay (Thermo Scientific). Equal amounts of protein were separated by SDS-polyacrylamide gel electrophoresis (SDS-PAGE) and electrophoretically transferred to PVDF membranes (Millipore, Billerica, MD). The membranes were then blocked with 5% skim milk and incubated with anti-NFAT1 (1:1000, Abcam), anti-ITGA6 (1:500, Proteintech, Chicago, USA), anti-E-cadherin (1:500, BD Biosciences), anti-Vimentin (1:500, BD Biosciences), or anti- α -tubulin (1:1000, Proteintech) primary antibody overnight at 4°C. The species-matched secondary antibodies were then incubated at room temperature for 1 hour and the proteins were detected by enhanced chemiluminescence (Thermo Scientific).

Wound Healing Assay

Cells were seeded onto 6-well culture plates and cultured to a subconfluent state in complete medium. After 24 h starvation in serum-free medium, cell monolayers were linearly scraped with a P-200 pipette tip. Cells that had detached from the bottom of the wells were gently aspirated and the remaining cells were incubated in serum-free medium. The width of the scratch was monitored under a microscope and quantified in terms of the difference between the original width of the wound and the width after cell migration.

Migration and Invasion Assays

Transwell plates (8- μm pores) (Costar/Corning, Lowell, MA) were used for the Transwell migration or invasion assays. 5×10^4 or 1×10^5 cells resuspended in serum-free medium were placed in the upper chamber of each insert, either uncoated or coated with Matrigel (BD Biosciences). The lower chamber contained culture medium with 10% FBS to act as a chemoattractant. The cells were incubated for 12 h or 24 h, and were then fixed and stained. Cells on the undersides of the filters were observed and counted under 200 \times magnification.

Cell Proliferation and Colony Formation Assays

For the CCK-8 assay, cells (1×10^3) were seeded into 96-well plates, incubated for 0–4 days, stained with 10 μl CCK-8 (Dojindo, Japan), and incubated for 2 h. Afterwards, absorbance at 450 nm was measured. For the colony formation assay, cells (0.3×10^3) were seeded into 6-well plates, cultured for 1 or 2 weeks, and the colonies then fixed in methanol, stained with crystal violet, and counted.

GSEA Analysis

Gene Set Enrichment Analysis (GSEA) was performed as previously described [2]. A microarray dataset (GSE12452) deposited

in the Gene Expression Omnibus (GEO) was applied to identify the association of *NFAT1* expression with EMT gene signature.

Immunofluorescence

Immunofluorescence analysis was performed as described previously [21]. Briefly, cells were fixed and incubated with the primary antibodies E-cadherin (610,181, 1:500, BD Biosciences) or Vimentin (610,193, 1:500, BD Biosciences) overnight at 4°C. After washing with PBS, cells were then incubated with fluorescence-conjugated secondary antibody (Invitrogen). Images were captured after staining with DAPI solution.

Chromatin Immunoprecipitation Assays

An EZ-Magna ChIP kit (Millipore, Billerica, MD) was used to perform the ChIP assay according to the manufacturer's instructions. In brief, cells were harvested for cross-linking and sheared by

sonication. The resultant chromatin fraction was immunoprecipitated using anti-HA (Abcam, ab9110) or negative control anti-IgG (Sigma) antibody. The DNA fragments were subsequently isolated using Qiagen MinElute column purification. 1 µg of ChIP DNA was used for ChIP-seq library preparation using Mondrian and directed to 50 bp sequencing using HiSeq 2500 (The Beijing Genomics Institute, China). ChIP quantitative PCR was performed using specific primers (GENEWIZ, China) (Table S1).

Luciferase Reporter Assays

pGL3 luciferase reporter plasmids containing wild type or mutant promoter of *ITGA6* were constructed. Cells were co-transfected with the indicated luciferase reporters (200 ng) and a pRL construct containing the Renilla luciferase reporter (1 ng), as well as NFAT1 overexpression plasmid or empty vector (2 µg). After 36 h, luciferase activity was

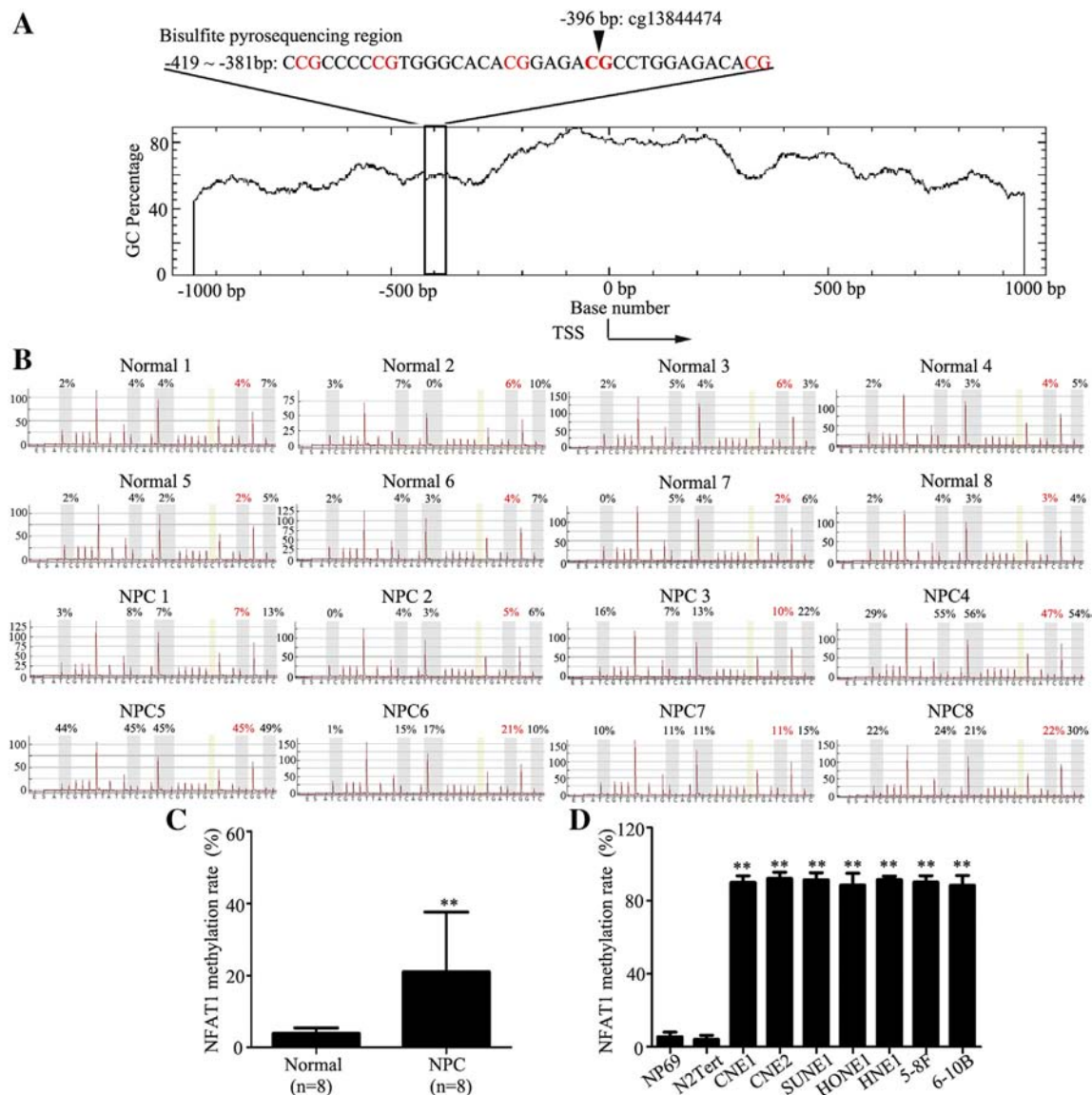


Figure 1. The *NFAT1* promoter is hypermethylated in NPC. (A) Schematic illustration of the *NFAT1* promoter CpG islands and bisulfite pyrosequencing region. TSS: transcription start site; cg13844474: CG site identified in our previous genome-wide methylation analysis; red text: CG sites for bisulfite pyrosequencing; bold red text: most significantly altered CG site in *NFAT1*. (B, C) Bisulfite pyrosequencing analysis of the *NFAT1* promoter region (B) and the average methylation levels (C) in normal ($n = 8$) and NPC ($n = 8$) tissues. Red text: cg13844474 CG site. (D) Bisulfite pyrosequencing analysis of *NFAT1* promoter region, as determined by bisulfite pyrosequencing analysis, in nasopharyngeal epithelial cell lines (NP69 and N2Tert) and NPC (CNE1, CNE2, SUNE1, HONE1, HNE1, 5-8F, and 6-10B) cell lines.

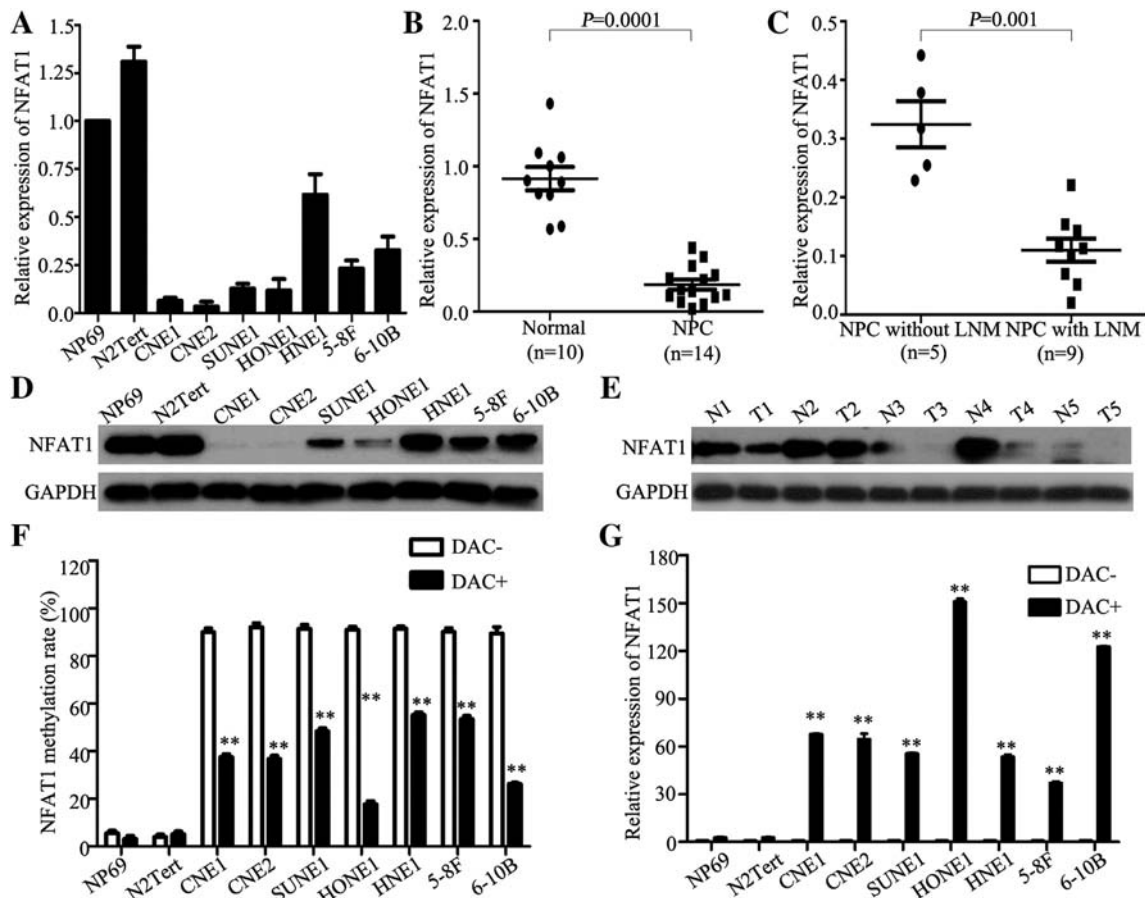


Figure 2. *NFAT1* promoter hypermethylation contributes to its down-regulation in NPC. (A, B) Quantitative RT-PCR analysis of *NFAT1* mRNA expression in normal nasopharyngeal epithelial cell lines (NP69 and N2Tert) and NPC cell lines (CNE1, CNE2, SUNE1, HONE1, HNE1, 5-8F, and 6-10B) (A), together with normal nasopharyngeal epithelial tissues ($n = 10$) and NPC tissues ($n = 14$) (B). (C) Relative expression of *NFAT1* in NPC patients without ($n = 5$) or with ($n = 9$) lymph node metastasis. (D, E) Western blot analysis of *NFAT1* protein in nasopharyngeal epithelial cell lines and NPC cell lines (D), normal nasopharyngeal epithelial tissues (N, $n = 5$) and NPC tissues (T, $n = 5$) (E). (F, G) *NFAT1* methylation levels were measured by bisulfite pyrosequencing analysis (F) and relative *NFAT1* mRNA levels were measured by real-time RT-PCR (G) with (DAC+) or without (DAC-) DAC treatment in nasopharyngeal epithelial cell lines and NPC cell lines. *P*-values were calculated using Student's *t*-test.

measured using the Dual luciferase Reporter Assay Kit (Promega). The value of firefly luciferase activity was normalized to the Renilla activity.

Popliteal Lymph Node Metastasis Model

All animal research protocols were approved by the Animal Care and Use Ethics Committee of Sun Yat-sen University Cancer Center. Twenty female BALB/c nude mice (4–5-weeks-old) were obtained from Charles River Laboratories (Beijing, China). Cells (3×10^5 in 0.1 mL of sterilized PBS) stably overexpressing *NFAT1* or vector were inoculated into the footpads of mice ($n = 10$ /group). The mice were sacrificed on day 28, and the primary tumors and popliteal lymph nodes were detached and paraffin-embedded. Then, sections of the primary tumors and lymph nodes were subjected to H&E staining for histological examination. Metastatic tumor cells in the lymph nodes were identified with an anti-pan-cytokeratin antibody (Thermo Scientific) and the images were captured using a NIKON ECLIPSE 80i microscope (Japan).

Immunohistochemistry (IHC)

Sections of primary tumors and popliteal lymph nodes were deparaffinized with xylene and rehydrated with a descending ethanol gradient. After treatment with citrate buffer, the sections were pre-

incubated with hydrogen peroxide, blocked with goat serum, incubated with primary antibodies (*NFAT1*, 1:100; ITGA6, 1:100; E-cadherin, 1:100; Vimentin, 1:100), and then labeled with an avidin-biotin peroxidase complex (Dako) followed by diaminobenzidine development (Sigma). Finally, sections were counterstained with hematoxylin, and images were captured using a NIKON ECLIPSE 80i microscope (Japan).

Statistical Analysis

Statistical analysis was performed with SPSS 18.0 (SPSS Inc.). Student's *t*-test (two-tailed) was used to compare means between two groups. All bars represent mean \pm SD derived from three independent experiments. *P* values $< .05$ were considered statistically significant. All data from this study has been deposited at Sun Yat-sen University Cancer Center for future reference (number RDDDB2018000416).

Results

The *NFAT1* Promoter is Hypermethylated in NPC

Our previous genome-wide methylation microarray (GSE52068) showed that *NFAT1* is one of the top-ranked hypermethylated

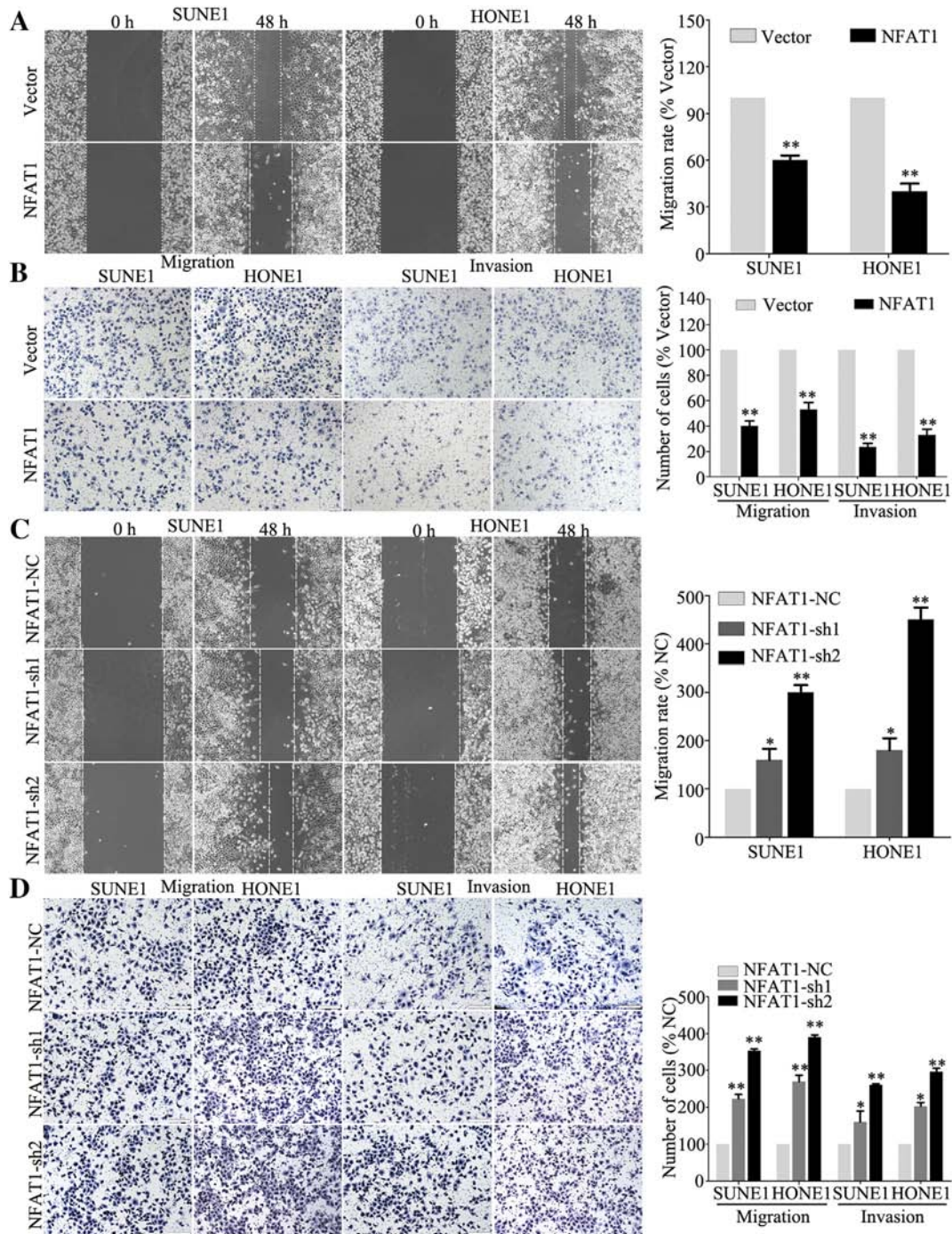


Figure 3. NFAT1 inhibits NPC cell migration and invasion *in vitro*. (A) Wound healing assays in SUNE1 and HONE1 cells stably overexpressing NFAT1 or empty vector. (B) Transwell migration and invasion assays with or without Matrigel. (C) Wound healing assay in SUNE1 and HONE1 cells transiently expressing control NC or *NFAT1*-shRNAs (sh-1 and sh-2). (D) Transwell migration and invasion assays with or without Matrigel. Magnification $\times 200$; scale bar, 100 μm . All experiments were repeated at least three times; data are mean \pm SD. *P*-values were calculated using Student's *t*-test.

transcription factor genes in NPC tissues, which was also identified in the Hong Kong dataset (GSE62336) (Figure S1). We validated the promoter methylation level of *NFAT1* by bisulfite pyrosequencing in independent NPC ($n = 8$) and normal tissues ($n = 8$). The CpG islands and region selected for bisulfite pyrosequencing in the *NFAT1* promoter region are shown in Figure 1A. The methylation level of *NFAT1* (cg13844474) in NPC tissues was significantly increased compared with normal tissues (Figure 1, B and C). Similarly, in NPC cell lines (CNE1, CNE2, SUNE1, HONE1, HNE1, 5-8F, and 6-

10B), the methylation level of *NFAT1* (cg13844474) was higher than that in normal nasopharyngeal epithelial cell lines (NP69 and N2Tert) (Figures 1D, S2). These results indicate that the *NFAT1* promoter is hypermethylated in NPC.

NFAT1 Down-Regulation is Associated With Its Promoter Hypermethylation

To understand the relationship between *NFAT1* expression and its promoter methylation status in NPC, we performed quantitative RT-

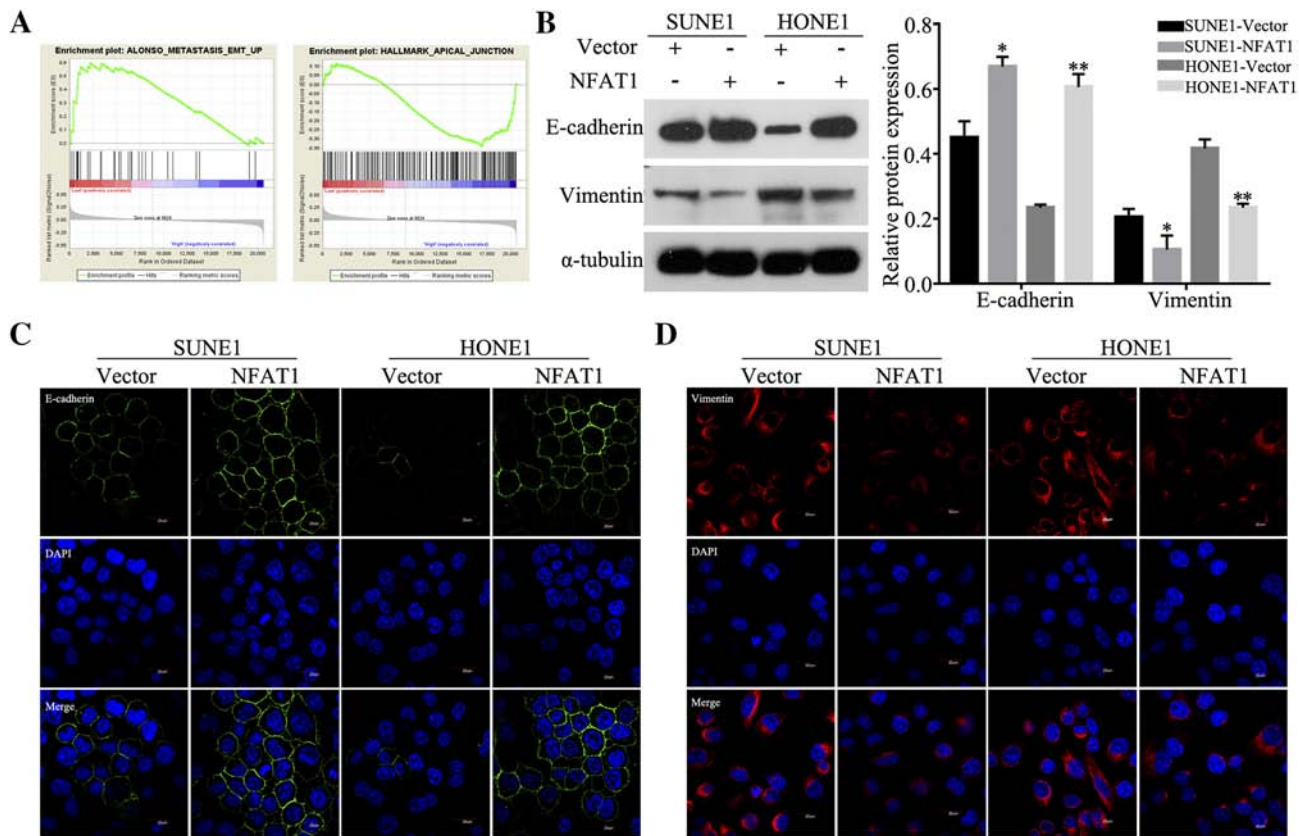


Figure 4. NFAT1 inhibits NPC cell epithelial-mesenchymal transition (EMT) *in vitro*. (A) GSEA enrichment plots revealed that enrichment of apical junction pathways was associated with down-regulation of *NFAT1*. (B) Western blot analysis of EMT marker (E-cadherin and Vimentin) expression levels in SUNE1 and HONE1 stably overexpressing vector or NFAT1. (C, D) Immunofluorescence staining of E-cadherin (C) and Vimentin (D) in SUNE1 and HONE1 cells with NFAT1 overexpression ($\times 400$).

PCR and found that *NFAT1* mRNA was significantly down-regulated in NPC cell lines and tissues, especially in those with lymph node metastasis (Figure 2, A–C). Furthermore, Western blot showed NFAT1 protein expression was down-regulated in both NPC cell lines and tissues (Figure 2, D and E). To determine whether the down-regulation of *NFAT1* results from its promoter hypermethylation, we treated immortalized normal nasopharyngeal epithelial cell lines and NPC cell lines with or without DAC. Bisulfite pyrosequencing and quantitative RT-PCR showed that *NFAT1* methylation levels were substantially decreased while *NFAT1* mRNA levels were significantly increased in NPC cell lines but not in normal nasopharyngeal epithelial cell lines (Figures 2, F and G, S2; $P < .05$). These findings suggest that *NFAT1* is down-regulated in NPC and that its down-regulation is associated with its promoter hypermethylation.

NFAT1 Inhibits NPC Cell Migration, Invasion, and EMT *In Vitro*

To investigate the role of *NFAT1* in NPC malignancy, we subjected SUNE1 and HONE1 cells stably overexpressing NFAT1 or the control vector to CCK8, colony formation, wound healing, and Transwell assays. Ectopic expression of NFAT1 significantly suppressed NPC cell migration (Figure 3, A and B) and invasion (Figure 3B). In contrast, silencing NFAT1 using two different shRNAs clearly increased the migratory and invasive abilities of NPC cells (Figures 3, C and D, S3, A–C). CCK8 and colony formation assays demonstrated that overexpression or silencing of NFAT1 had little effects on NPC cell viability and colony formation (Figure S3,

D–G). GSEA analysis based on the GSE12452 database showed that *NFAT1* was associated with EMT and hallmark apical junction (Figure 4A). Western blot and immunofluorescence staining showed that overexpression of NFAT1 was associated with increased expression of the epithelial marker E-cadherin and decreased expression of the mesenchymal marker Vimentin (Figure 4, B–D). Collectively, these findings indicate that NFAT1 suppresses NPC cell migration, invasion, and EMT *in vitro*.

NFAT1 Represses the Transcription of *ITGA6* in NPC

To identify target genes of NFAT1, ChIP-Seq was performed using HA tag antibody. Sequence motif search of the NFAT1-binding peaks showed greatest enrichment for the consensus NFAT1 motif (GGAAA) (Figure 5A). The peak intensity profile of these sites flanking the TSS is shown in Figure 5B, and a conservation analysis showed that sequences within and flanking the NFAT1 binding sites are evolutionarily conserved. To further identify downstream target genes of NFAT1, we performed Gene Ontology analysis and selected 10 genes for validation that overlapped among proteoglycans in cancer, regulation of cytoskeleton, cell adhesion, and focal adhesion (Figure 5C). Quantitative RT-PCR showed that *ITGA6* was among the most down-regulated genes associated with NFAT1 overexpression (Figure 5D). Correlation analysis further demonstrated that *ITGA6* mRNA expression inversely correlated with *NFAT1* mRNA expression in the GSE12452 database (Figure 5E; $R = -0.357$, $P < .05$).

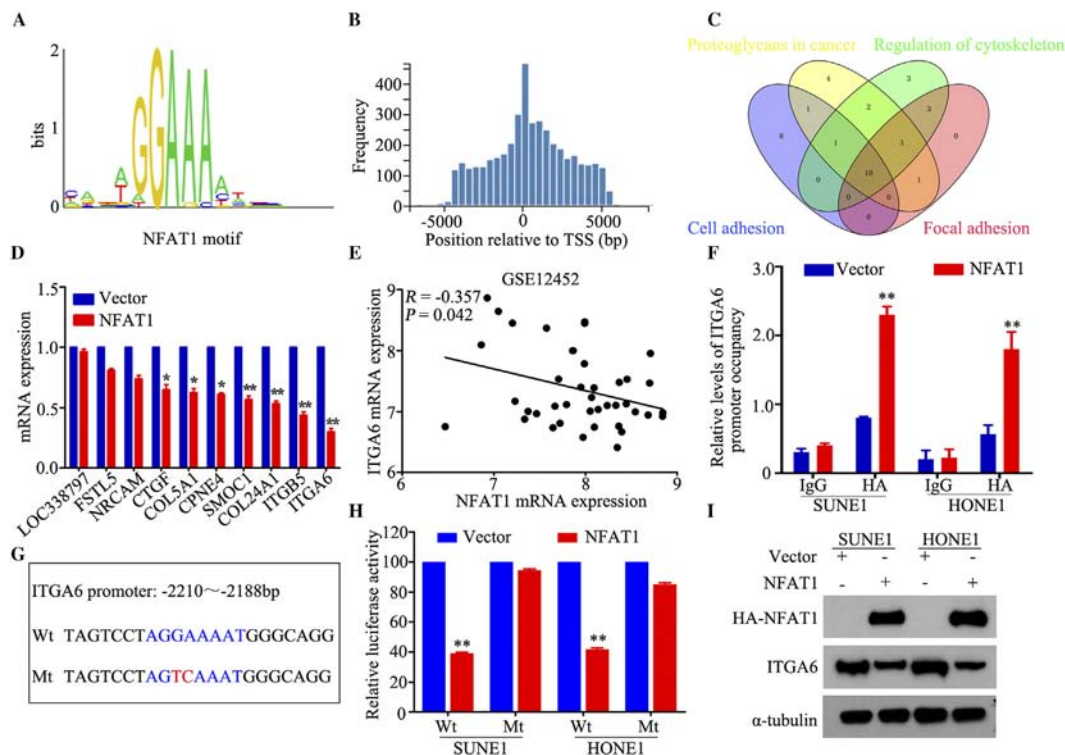


Figure 5. NFAT1 represses *ITGA6* transcription. (A) The top consensus sequence motif compiled from NFAT1-binding peaks centered on the binding summits. (B) The distribution of NFAT1 binding motif position relative to TSS. (C) Venn Diagram: Number of regulated genes in proteoglycans in cancer, regulation of cytoskeleton, cell adhesion, and focal adhesion. Note, 10 genes are commonly regulated in cancer and apical junction. (D) Validation of 10 differentially expressed genes by RT-PCR. (E) Correlations between *NFAT1* mRNA expression and *ITGA6* expression in GSE12452 dataset. (F) ChIP real-time PCR assays were conducted to assess the enrichment of NFAT1 in the *ITGA6* promoter region in NFAT1 overexpressing NPC cells. Data are means \pm standard deviation. $**P < .01$ compared with IgG; Student's *t*-tests. (G) Wild type (Wt) or mutant (Mt) *NFAT1* target sequence of the *ITGA6* promoter. (H) Relative luciferase activity of the vector or NFAT1 overexpressing NPC cells after transfection with Wt or Mt. *ITGA6* promoter reporter genes. All experiments were repeated at least three times; data are means \pm standard deviation. *P*-values were calculated using Student's *t*-test. (I) Western blot analysis of *ITGA6* expression in the vector or NFAT1 overexpressing NPC cells.

ChIP real-time PCR assay using an anti-HA antibody confirmed that restoration of NFAT1 increased the occupancy of NFAT1 at the *ITGA6* promoter region (Figure 5F). A luciferase reporter gene assay was performed to determine whether *ITGA6* is a direct target of NFAT1. We cloned the wild type or mutant *NFAT1* target sequences of the *ITGA6* promoter into luciferase reporter vectors (Figure 5G). After co-transfection with *NFAT1* plasmids, the luciferase activity of the *ITGA6* reporter gene was significantly reduced, whereas the activity of the mutant reporter gene was not affected (Figure 5H), confirming that NFAT1 can bind to the *ITGA6* promoter. Western blot further showed that overexpression of NFAT1 significantly reduced *ITGA6* protein expression. Taken together, these findings suggest that NFAT1 can negatively regulate *ITGA6* expression by repressing the transcription of *ITGA6*.

ITGA6 is a Functional Target of NFAT1 in NPC

To determine whether NFAT1-mediated *ITGA6* down-regulation contributed to its inhibitory effect on NPC cell migration and invasion, we restored *ITGA6* expression in NPC cells stably overexpressing NFAT1. Co-transfection with *ITGA6* significantly abolished the inhibitory effects of NFAT1 on NPC cell migration and invasion (Figure 6, A–D). In addition, the expression level of E-cadherin induced by NFAT1 was substantially decreased, and Vimentin was clearly increased following co-transfection with

ITGA6 (Figure 6, E and F). These findings demonstrate that *ITGA6* is a functional target of NFAT1 in NPC cells.

NFAT1 Inhibits NPC Aggressiveness In Vivo

To determine whether NFAT1 affects NPC metastasis *in vivo*, we established a popliteal lymph node metastasis mouse model by inoculating the footpads of nude mice with HONE1 cells stably overexpressing NFAT1 or vector alone (Figure 7A). H&E staining showed that primary tumors in the NFAT1 overexpression group exhibited sharp edges that expanded as spheroids, indicating a less aggressive phenotype with invasion towards the skin and muscle (Figure 7B). Furthermore, the popliteal lymph node volumes were smaller, and pan-cytokeratin-positive tumor cells were fewer in the NFAT1 overexpression group than in the vector group (Figure 7, C–E). Taken together, these findings imply that NFAT1 suppresses NPC cell metastasis *in vivo*.

To further examine whether NFAT1 suppresses *ITGA6* expression *in vivo*, IHC was used to assess NFAT1 and *ITGA6* protein levels in primary tumors. *ITGA6* expression was significantly decreased in the NFAT1 overexpression group compared with the vector group (Figure 7F). In addition, overexpression of NFAT1 increased E-cadherin expression, but decreased Vimentin expression. In summary, these results suggest that NFAT1 up-regulation is associated with a reduction in *ITGA6* expression *in vivo*.

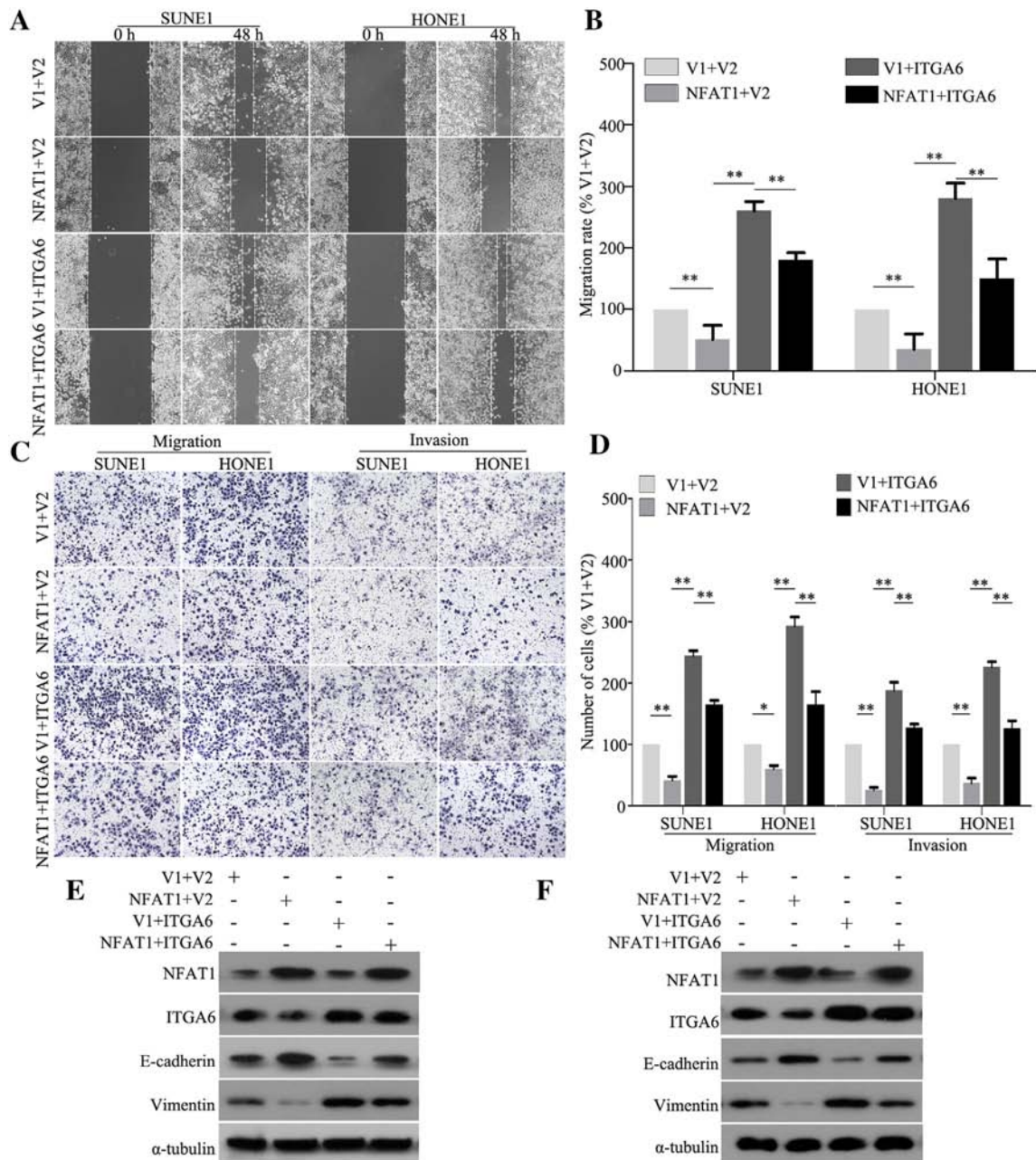


Figure 6. *ITGA6* is a functional target of NFAT1 in NPC. *ITGA6* plasmid was transfected in SUNE1 and HONE1 cells stably overexpressing NFAT1 or the empty vector (V) (A, B) Wound healing assay. (C, D) Transwell migration and invasion assays with or without Matrigel. (E, F) E-cadherin, Vimentin, ITGA6 and NFAT1 expression levels were measured via Western blot. All experiments were repeated at least three times; data are means \pm standard deviation. *P*-values were calculated using Student's *t*-test.

Discussion

This study identified the novel role of NFAT1 in NPC progression. Our findings establish that NFAT1 down-regulation in NPC is associated with its promoter hypermethylation. Restoration of NFAT1 significantly suppressed epithelial-mesenchymal transition and metastasis *in vitro* and *in vivo*. The tumor suppressor role of NFAT1 might depend on its transcriptional repression of *ITGA6*. Overall, our findings uncovered a novel mechanism by which NFAT1 regulates *ITGA6* expression and its role in NPC progression.

DNA methylation, one of the best characterized epigenetic alterations, can lead to long-term repression of gene expression [22]. Approximately sixty percent of genes have one or more CpG

islands in their promoter and can therefore be potentially silenced by DNA methylation. DNA methylation patterns are largely modified in cancer cells and the alteration of DNA methylation patterns is a hallmark of cancer [23]. Numerous studies have found that repression of tumor suppressor genes (TSGs) by DNA hypermethylation contributes to dysregulation of various cellular pathways (cell cycle, apoptosis, and metastasis) during carcinogenesis [24–26]. Our previous genome-wide methylation microarray study showed that DNA hypermethylation is frequent in NPC [14], and that *NFAT1* was one of the most differentially hypermethylated transcriptional factor genes in NPC tissues. However, the function and mechanism of NFAT1 in NPC remained unclear.

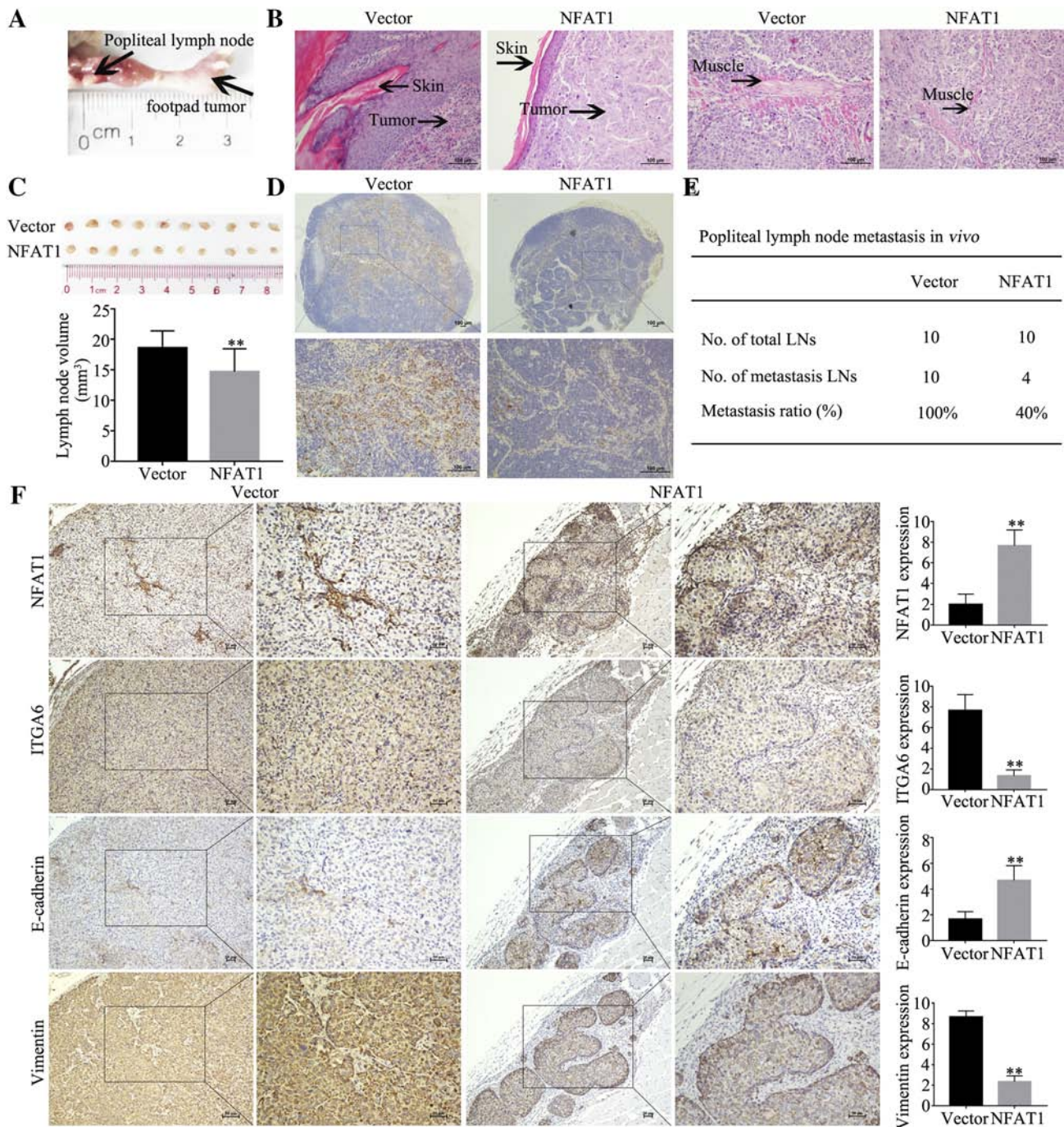


Figure 7. NFAT1 suppresses NPC aggressiveness *in vivo*. HONE1 cells stably overexpressing NFAT1 or empty vector ($n = 10$ per group) were injected into the footpads of mice to construct inguinal lymph node metastasis models. (A) Representative images of primary footpad tumor and metastatic popliteal lymph node. (B) Representative images of microscopic primary tumors in the footpad stained with hematoxylin and eosin (H&E). Magnification $\times 200$; scale bar, $100 \mu\text{m}$. (C) Representative images and quantification of the average volumes of the popliteal lymph nodes. Mean \pm standard deviation; $**P < .01$ compared with vector; Student's *t*-test. (D) Immunohistochemical staining for pan-cytokeratin-positive tumor cells in popliteal lymph nodes ($\times 4$ and $\times 200$). Scale bar, $100 \mu\text{m}$. (E) Metastatic ratios of popliteal lymph nodes; Chi-squared test. (F) Immunohistochemical staining for NFAT1, ITGA6, E-cadherin, and Vimentin in primary footpad tumors ($\times 100$ and $\times 200$). Each mouse sample was considered as an independent experiment; three technological replicates were repeated in each sample.

NFAT1, one member of the NFAT family, is a transcription factor that has profound effects on the proliferation and migration of T cells [27]. All NFAT family proteins share a highly conserved Rel-homology domain (RHD), which endows the NFAT members with a common DNA-binding specificity [28]. In addition, these calcium-

responsive NFAT isoforms (NFAT1-NFAT4) have another conserved NFAT homology domain (NHD), which can bind to promoter elements and initiate gene transcription. Recent studies suggest that NFATs may be involved in many aspects of cancer, including cancer cell survival [29,30], apoptosis [31–34], migration

and metastasis [35–37], angiogenesis [38–40], and the tumor microenvironment [41]. There is little knowledge regarding the role that NFAT1 plays in NPC. In this study, we demonstrated that *NFAT1* is significantly down-regulated in NPC tissues and cell lines as a result of promoter hypermethylation. Overexpression of NFAT1 inhibited NPC cell migration, invasion, EMT, and metastasis, but had little influence on cell proliferation. Therefore, we conclude that NFAT1 acts as a tumor suppressor in NPC progression, a role which has also been described for NFAT1 in glioma [42]. It has been reported that NFAT1 functions as an oncogene in melanoma [43], indicating that NFAT1 exerts different functions in different tumor types.

EMT is a normal physiological process during which epithelial cells acquire enhanced motility and invasiveness typical of mesenchymal cells. Recent studies suggest that multiple morphogenic and environmental signals, such as transforming growth factor- β (TGF- β), WNT, epidermal growth factors and platelet-derived growth factors, inflammatory cytokines, and integrin receptor ligands all promote EMT [2,21,44,45]. After screening downstream NFAT1 targets, we found that expression of *ITGA6* is the most significantly affected by NFAT1. Consistent with this observation, we found that NFAT1 could directly bind to the promoter region of *ITGA6* and inhibit its transcription. *ITGA6*, an extracellular integrin receptor, could promote EMT and invasive and metastatic behavior in carcinoma progression [46,47]. Restoration of normal *ITGA6* levels in NPC cells via NFAT1 overexpression significantly reversed the inhibitory effects of NFAT1 on migration, invasion, and EMT, indicating that *ITGA6* is a functional target of NFAT1 in NPC.

Conclusions

In summary, we report that *NFAT1* is epigenetically silenced by promoter methylation in NPC. Epigenetic silencing of *NFAT1* promotes EMT and metastasis in NPC by activating *ITGA6* transcription. These findings underscore the significant role of NFAT1 as well as *ITGA6* in NPC metastasis, and provide a specific target for the development of novel therapeutic strategies for patients with metastatic NPC in the future.

Supplementary data to this article can be found online at <https://doi.org/10.1016/j.neo.2019.01.006>.

Author contributions

N.L. and J.Z. designed the research. J.Z., Z.Z., P.Z., and Y.L. conducted the experiments. J.Z., Y.Y., Y.W., X.T., X.W., X.H., Y.L., Y.S., and J.M. acquired and analyzed the data. N.L., J.M., Q.H., and X.Y. provided the reagents. J. Z. and N.L. wrote the manuscript. All authors read and approved the final manuscript.

References

- [1] Cao SM, Simons MJ, and Qian CN (2011). The prevalence and prevention of nasopharyngeal carcinoma in China. *Chin J Cancer* **30**, 114–119.
- [2] Zhang J, Wen X, Liu N, Li YQ, Tang XR, Wang YQ, He QM, Yang XJ, Zhang PP, and Ma J, et al (2017). Epigenetic mediated zinc finger protein 671 downregulation promotes cell proliferation and tumorigenicity in nasopharyngeal carcinoma by inhibiting cell cycle arrest. *J Exp Clin Cancer Res* **36**, 147.
- [3] Torre LA, Bray F, Siegel RL, Ferlay J, Lortet-Tieulent J, and Jemal A (2015). Global cancer statistics, 2012. *CA Cancer J Clin* **65**, 87–108.
- [4] Lai SZ, Li WF, Chen L, Luo W, Chen YY, Liu LZ, Sun Y, Lin AH, Liu MZ, and Ma J (2011). How does intensity-modulated radiotherapy versus conventional two-dimensional radiotherapy influence the treatment results in nasopharyngeal carcinoma patients? *Int J Radiat Oncol Biol Phys* **80**, 661–668.
- [5] Ghavifekr FM, Farshdousti HM, Shانهbandi D, and Baradaran B (2013). DNA methylation pattern as important epigenetic criterion in cancer. *Genet Res Int* **2013**, 317569.
- [6] Ma X, Wang YW, Zhang MQ, and Gazdar AF (2013). DNA methylation data analysis and its application to cancer research. *Epigenomics* **5**, 301–316.
- [7] Shakeri H, Fakhrou A, Nikanfar A, and Mohaddes-Ardebili SM (2016). Methylation Analysis of BRCA1 and APC in Breast Cancer and It's Relationship to Clinicopathological Features. *Clin Lab* **62**, 2333–2337.
- [8] Jiang D, Shen Y, Dai D, Xu Y, Xu C, Zhu H, Huang T, and Duan S (2014). Meta-analyses of methylation markers for prostate cancer. *Tumour Biol* **35**, 10449–10455.
- [9] Kajiura K, Masuda K, Naruto T, Kohmoto T, Watabnabe M, Tsuboi M, Takizawa H, Kondo K, Tangoku A, and Imoto I (2017). Frequent silencing of the candidate tumor suppressor TRIM58 by promoter methylation in early-stage lung adenocarcinoma. *Oncotarget* **8**, 2890–2905.
- [10] Wang N, Sui F, Ma J, Su X, Liu J, Yao D, Shi B, Hou P, and Yang Q (2016). Site-specific Hypermethylation of RUNX3 Predicts Poor Prognosis in Gastric Cancer. *Arch Med Res* **47**, 285–292.
- [11] Li LL, Shu XS, Wang ZH, Cao Y, and Tao Q (2011). Epigenetic disruption of cell signaling in nasopharyngeal carcinoma. *Chin J Cancer* **30**, 231–239.
- [12] Li L, Zhang Y, Guo BB, Chan FK, and Tao Q (2014). Oncogenic induction of cellular high CpG methylation by Epstein-Barr virus in malignant epithelial cells. *Chin J Cancer* **33**, 604–608.
- [13] Dai W, Cheung AK, Ko JM, Cheng Y, Zheng H, Ngan RK, Ng WT, Lee AW, Yau CC, and Lee VH, et al (2015). Comparative methylome analysis in solid tumors reveals aberrant methylation at chromosome 6p in nasopharyngeal carcinoma. *Cancer Med* **4**, 1079–1090.
- [14] Ren X, Yang X, Cheng B, Chen X, Zhang T, He Q, Li B, Li Y, Tang X, and Wen X, et al (2017). HOPX hypermethylation promotes metastasis via activating SNAIL transcription in nasopharyngeal carcinoma. *Nat Commun* , 14053.
- [15] Baksh S, Widlund HR, Frazer-Abel AA, Du J, Fosmire S, Fisher DE, DeCaprio JA, Modiano JF, and Burakoff SJ (2002). NFATc2-mediated repression of cyclin-dependent kinase 4 expression. *Mol Cell* **10**, 1071–1081.
- [16] Carvalho LD, Teixeira LK, Carrossini N, Caldeira AT, Ansel KM, Rao A, and Viola JP (2007). The NFAT1 transcription factor is a repressor of cyclin A2 gene expression. *Cell Cycle* **6**, 1789–1795.
- [17] Viola JP, Carvalho LD, Fonseca BP, and Teixeira LK (2005). NFAT transcription factors: from cell cycle to tumor development. *Braz J Med Biol Res* **38**, 335–344.
- [18] Robbs BK, Cruz AL, Werneck MB, Mognol GP, and Viola JP (2008). Dual roles for NFAT transcription factor genes as oncogenes and tumor suppressors. *Mol Cell Biol* **28**, 7168–7181.
- [19] Cao K, Wang G, Li W, Zhang L, Wang R, Huang Y, Du L, Jiang J, Wu C, and He X, et al (2015). Histone deacetylase inhibitors prevent activation-induced cell death and promote anti-tumor immunity. *Oncogene* **34**, 5960–5970.
- [20] Kaunisto A, Henry WS, Montaser-Kouhsari L, Jaminet SC, Oh EY, Zhao L, Luo HR, Beck AH, and Toker A (2015). NFAT1 promotes intratumoral neutrophil infiltration by regulating IL8 expression in breast cancer. *Mol Oncol* **9**, 1140–1154.
- [21] Zhang J, Wen X, Ren XY, Li YQ, Tang XR, Wang YQ, He QM, Yang XJ, Sun Y, and Liu N, et al (2016). YPEL3 suppresses epithelial-mesenchymal transition and metastasis of nasopharyngeal carcinoma cells through the Wnt/beta-catenin signaling pathway. *J Exp Clin Cancer Res* **35**, 109.
- [22] Bird A (2002). DNA methylation patterns and epigenetic memory. *Genes Dev* **16**, 6–21.
- [23] Rossodivita AA, Boudoures AL, Mecoli JP, Steenkiste EM, Karl AL, Vines EM, Cole AM, Ansbros MR, and Thompson JS (2014). Histone H3 K79 methylation states play distinct roles in UV-induced sister chromatid exchange and cell cycle checkpoint arrest in *Saccharomyces cerevisiae*. *Nucleic Acids Res* **42**, 6286–6299.
- [24] Dhami GK, Liu H, Galka M, Voss C, Wei R, Muranko K, Kaneko T, Cregan SP, Li L, and Li SS (2013). Dynamic methylation of Numb by Set8 regulates its binding to p53 and apoptosis. *Mol Cell* **50**, 565–576.
- [25] Liu Z, Zhang J, Gao Y, Pei L, Zhou J, Gu L, Zhang L, Zhu B, Hattori N, and Ji J, et al (2014). Large-scale characterization of DNA methylation changes in human gastric carcinomas with and without metastasis. *Clin Cancer Res* **20**, 4598–4612.
- [26] Abou-Elhamd KE and Habib TN (2007). The flow cytometric analysis of premalignant and malignant lesions in head and neck squamous cell carcinoma. *Oral Oncol* **43**, 366–372.
- [27] Jain J, Burgeon E, Badalian TM, Hogan PG, and Rao A (1995). A similar DNA-binding motif in NFAT family proteins and the Rel homology region. *J Biol Chem* **270**, 4138–4145.

- [28] Irnaten M, Zhdanov A, Brennan D, Crotty T, Clark A, Papkovsky D, and O'Brien C (2018). Activation of the NFAT-Calcium Signaling Pathway in Human Lamina Cribrosa Cells in Glaucoma. *Invest Ophthalmol Vis Sci* **59**, 831–842.
- [29] Ram BM, Dolpady J, Kulkarni R, Usha R, Bhorla U, Poli UR, Islam M, Trehanpati N, and Ramakrishna G (2018). Human papillomavirus (HPV) oncoprotein E6 facilitates Calcineurin-Nuclear factor for activated T cells 2 (NFAT2) signaling to promote cellular proliferation in cervical cell carcinoma. *Exp Cell Res* **362**, 132–141.
- [30] Lu WC, Xie H, Tie XX, Wang R, Wu AH, and Shan FP (2018). NFAT-1 hyperactivation by methionine enkephalin (MENK) significantly induces cell apoptosis of rats C6 glioma *in vivo* and *in vitro*. *Int Immunopharmacol* **56**, 1–8.
- [31] Mane SD, Thoh M, Sharma D, Sandur SK, and Naidu KA (2016). Ascorbyl Stearate Promotes Apoptosis Through Intrinsic Mitochondrial Pathway in HeLa Cancer Cells. *Anticancer Res* **36**, 6409–6417.
- [32] Mognol GP, Carneiro FR, Robbs BK, Faget DV, and Viola JP (2016). Cell cycle and apoptosis regulation by NFAT transcription factors: new roles for an old player. *Cell Death Dis* **7**, e2199.
- [33] Yiu GK, Kaunisto A, Chin YR, and Toker A (2011). NFAT promotes carcinoma invasive migration through glypican-6. *Biochem J* **440**, 157–166.
- [34] Yiu GK and Toker A (2006). NFAT induces breast cancer cell invasion by promoting the induction of cyclooxygenase-2. *J Biol Chem* **281**, 12210–12217.
- [35] Yoeli-Lerner M, Chin YR, Hansen CK, and Toker A (2009). Akt/protein kinase b and glycogen synthase kinase-3beta signaling pathway regulates cell migration through the NFAT1 transcription factor. *Mol Cancer Res* **7**, 425–432.
- [36] Zhao X, Liu J, Feng L, Ge S, Yang S, Chen C, Li X, Peng L, Mu Y, and Wang Y, et al (2018). Anti-angiogenic effects of Qingdu granule on breast cancer through inhibiting NFAT signaling pathway. *J Ethnopharmacol* **10**, 261–269.
- [37] Zhao X, Wang Q, Yang S, Chen C, Li X, Liu J, Zou Z, and Cai D (2016). Quercetin inhibits angiogenesis by targeting calcineurin in the xenograft model of human breast cancer. *Eur J Pharmacol* **781**, 60–68.
- [38] Suehiro J, Kanki Y, Makihara C, Schadler K, Miura M, Manabe Y, Aburatani H, Kodama T, and Minami T (2014). Genome-wide approaches reveal functional vascular endothelial growth factor (VEGF)-inducible nuclear factor of activated T cells (NFAT) c1 binding to angiogenesis-related genes in the endothelium. *J Biol Chem* **289**, 29044–29059.
- [39] Mena MP, Papiewska-Pajak I, Przygodzka P, Kozaczuk A, Boncela J, and Cierniewski CS (2014). NFAT2 regulates COX-2 expression and modulates the integrin repertoire in endothelial cells at the crossroads of angiogenesis and inflammation. *Exp Cell Res* **324**, 124–136.
- [40] Shou J, Jing J, Xie J, You L, Jing Z, Yao J, Han W, and Pan H (2015). Nuclear factor of activated T cells in cancer development and treatment. *Cancer Lett* **361**, 174–184.
- [41] Zhang J, Tian XJ, and Xing J (2016). Signal Transduction Pathways of EMT Induced by TGF-beta, SHH, and WNT and Their Crosstalks. *J Clin Med* **5**.
- [42] Han S, Meng L, Jiang Y, Cheng W, Tie X, Xia J, and Wu A (2017). Lithium enhances the antitumour effect of temozolomide against TP53 wild-type glioblastoma cells via NFAT1/FasL signalling. *Br J Cancer* **116**, 1302–1311.
- [43] Shoshan E, Brauer RR, Kamiya T, Mobley AK, Huang L, Vasquez ME, Velazquez-Torres G, Chakravarti N, Ivan C, and Prieto V, et al (2016). NFAT1 Directly Regulates IL8 and MMP3 to Promote Melanoma Tumor Growth and Metastasis. *Cancer Res* **76**, 3145–3155.
- [44] Lindsey S and Langhans SA (2014). Crosstalk of Oncogenic Signaling Pathways during Epithelial-Mesenchymal Transition. *Front Oncol* **4**, 358.
- [45] Gan L, Meng J, Xu M, Liu M, Qi Y, Tan C, Wang Y, Zhang P, Weng W, and Sheng W, et al (2018). Extracellular matrix protein 1 promotes cell metastasis and glucose metabolism by inducing integrin beta4/FAK/SOX2/HIF-1alpha signaling pathway in gastric cancer. *Oncogene* **37**, 744–755.
- [46] Brooks DL, Schwab LP, Krutilina R, Parke DN, Sethuraman A, Hoogewijs D, Schorg A, Gotwald L, Fan M, and Wenger RH, et al (2016). ITGA6 is directly regulated by hypoxia-inducible factors and enriches for cancerstem cell activity and invasion in metastatic breast cancer models. *Mol Cancer* **15**, 26.
- [47] Zhang K, Myllymaki SM, Gao P, Devarajan R, Kytola V, Nykter M, Wei GH, and Manninen A (2017). Oncogenic K-Ras upregulates ITGA6 expression via FOSL1 to induce anoikis resistance and synergizes with alphaV-Class integrins to promote EMT. *Oncogene* **36**, 5681–5694.